RSC Advances

RSC Publishing

COMMUNICATION

Engineered osmosis for pre-concentration of sugar-derived biofuels†

Cite this: *RSC Advances*, 2013, **3**, 11467

Received 5th March 2013,
Accepted 7th May 2013

DOI: 10.1039/c3ra41075g

www.rsc.org/advances

Guy Z. Ramon,[ab] Yerucham Naaman[a] and Carlos G. Dosoretz*[a]

A novel process is proposed for the pre-concentration of sugar-derived biofuels from an aqueous fermentation broth, using Engineered Osmosis, an emerging membrane technology. While in itself an interesting candidate for such applications, the outlined scheme is unique in that it utilizes an energy source inherent to such systems, namely the osmotic potential which exists between the stock solution (glucose) and the dilute fermentation product.

Biofuels produced through fermentation of sugar, *e.g.* ethanol and butanol, are leading candidates for use as renewable transportation fuels.[1–4] However, a main obstacle to obtaining a high overall energy efficiency in their production is their relatively low concentration in the aqueous fermentation broth. For example, the concentration of butanol is normally ~2 wt%.[4,5] This dilute stream must be separated, for example using distillation, and the energy consumption increases dramatically for more dilute initial composition. In fact, a cut-off initial composition, for which the energy for separation is equal to that stored in the fuel, is estimated to be ~2% and ~1% for ethanol and butanol, respectively.[4,6] Hybrid separation processes involving some combination of distillation, pervaporation, gas stripping and adsorption have also been suggested but it appears there is no clearly established operational pathway for this separation yet.[6–9] Clearly, whatever the ultimate combination of separation technologies, it is most desirable to increase the initial concentration of the product prior to separation.

In this communication we describe a novel scheme, which integrates an Engineered Osmosis (EO) membrane contactor[10,11] into a biofuel production process based on glucose fermentation (see schematic drawing in Fig. 1). During this pre-concentration stage, the existing osmotic potential of the undiluted sugar stock solution is used to drive water out of the biofuel-water mixture. Essentially, the EO unit brings into contact, through an osmotic membrane, the concentrated glucose feed (at concentrations of ~1–2 M) with the fermentation product (here taken as butanol at a concentration of 2% by weight). The glucose solution has a higher molar concentration and thus acts as an osmotic 'draw', driving water permeation through the membrane. This results in simultaneous concentration of the biofuel stream and dilution of the glucose stream, to an extent that is dependent on various process parameters affecting mass transfer and the available membrane area.

The process achieves a double objective: a first step concentration of the product as well as partial or complete dilution of the concentrated feedstock to the desired pre-fermentation concentration. A limitation inherent to the process is imposed by the concentration of the 'draw' solution, the driving force for the process. As the stock solution is diluted and the feed is concentrated, the permeation may become prohibitively low. However, the advantage here is in the potential for energy savings in the costly first-step concentration of a dilute stream, through the utilization of an energy source *inherently present* in the system. Concentrating a butanol solution two-fold, to ~4 wt%, results in a

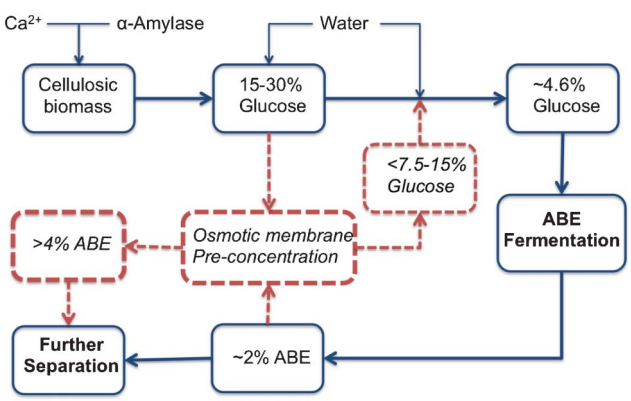

Fig. 1 Process schematic, illustrating a standard pathway for producing sugar-derived biofuels (blue), and the integrated, osmotic membrane pre-concentration step (red, dashed). ABE: acetone, butanol, ethanol.

[a]*Department of Civil & Environmental Engineering, Technion-IIT, Haifa 32000, Israel. E-mail: carlosd@technion.ac.il*
[b]*Department of Mechanical & Aerospace Engineering, Princeton University, Princeton, NJ 08544, USA*

† Electronic supplementary information (ESI) available: Model parameters, additional calculations, experimental system description. See DOI: 10.1039/c3ra41075g

corresponding reduction in the energy of separation—roughly from ~22 MJ kg^{-1} or ~60% of the available energy, to ~10 MJ kg^{-1}, which is ~28% of the energy.[6]

In what follows, a process model is used to provide some quantitative indication of the main performance parameters of the proposed process, particularly the permeation rate and energy consumption. In doing so, certain assumptions must be made, primarily due to inherent uncertainties related to the exact process configuration. The EO process is essentially a mass exchanger, where two streams are contacted through a membrane. In the case considered, a concentrated glucose solution is pumped on one side of the membrane, while the butanol mixture is pumped on the other side. The glucose solution, having a larger osmotic pressure, acts as the 'draw' and induces permeation of water from the butanol mixture (the 'feed') through the membrane. The exchange of water results in the simultaneous concentration of the feed and dilution of the draw, so that the driving force for water transport will diminish as the two solutions are contacted, eventually terminating at the point where the osmotic pressure equilibrates across the membrane. It is impractical to proceed until such equilibration is achieved and some compromise must be sought through optimization of membrane area requirements and the desired concentration of diluted glucose solution prior to fermentation.

Process model equations

A straightforward, global mass balance over a membrane module, accounting for both feed and draw streams, requires that

$$c_{G,i}Q_{G,i} = c_{G,o}(Q_{G,i} + J_wA_m) \quad (1a)$$

and

$$c_{B,i}Q_{B,i} = c_{B,o}(Q_{B,i} - J_wA_m), \quad (1b)$$

in which c is the concentration, Q is the volumetric flow rate, J_w is the water flux through the membrane, A_m is the membrane surface area and the subscripts G, B, i, and o denote glucose, butanol, inlet and outlet, respectively. Implicit in these expressions is that leakage of either solute (*i.e.* glucose and butanol) through the membrane is negligibly small. This assumption is made for the sake of simplicity and may be readily relaxed if the solute permeabilities are known. Further assuming that the flow rates on the feed and draw sides are equal, *i.e.* $Q_{B,i} = Q_{G,i} = Q$, eqn (1a) and (b) may be combined to yield

$$\mathrm{CF} = \frac{Q}{Q - J_wA_m}, \quad (2)$$

in which the concentration factor, $\mathrm{CF} = c_{B,o}/c_{B,i}$, has been defined, reflecting the degree of concentration achieved in the system. Finally, the water flux through the membrane is given by

$$J_w = A(\pi_{G,m} - \pi_{B,m}) \quad (3)$$

where A is the membrane water permeability, and π_G, π_B, denote the osmotic pressure of the glucose and butanol solutions, respectively. The subscript m indicates that the osmotic pressure is taken at the membrane–solution interface. In this system, the inlet conditions are known parameters. The system performance may generally be calculated by imposing outlet concentrations, *i.e.*, dictating a degree of concentration from which a required membrane area is then inferred; conversely, given a membrane surface area, one may calculate the compositions at the outlet.

In eqn (3), describing the osmotic water flux, the osmotic pressure is taken at the membrane surface, since it is usually quite different to that in the bulk solution due to concentration polarization (CP). Depending on the direction of the water flux, CP may result in either accumulation or dilution of the solute at the membrane surface, whence it is referred to as either concentrative or dilutive CP. Moreover, in EO polarization may occur in the feed stream, where it is referred to as 'external' CP, or within the membrane itself—'internal' CP.[10,11] Internal CP is caused due to the asymmetric structure of modern membranes, which are comprised of a thin selective skin or film, fabricated on top of a porous substrate imparting it with mechanical stability. Within this porous sub-structure, solute transport away from the membrane occurs solely through hindered molecular diffusion. This is in sharp contrast to the transport in the channel external to the membrane, where axial convection is facilitated by the flow of the bulk solution. Consequently, internal CP is usually the main cause for the observed reduction of the 'effective' osmotic pressure difference, which is lower than its full potential based on bulk concentrations. Assuming a linear concentration dependence of the osmotic pressure and, as before, a fully retentive membrane, the osmotic driving force is[12]

$$\Delta\pi_m = RT(c_{G,m} - c_{B,m}) = RT(c_{G,b}e^{-Jw/k} - c_{B,b}e^{JwS/D}). \quad (4)$$

Here, the subscript b denotes a bulk quantity, D is the molecular diffusion coefficient, R is the universal gas constant, T the absolute temperature, k is the mass transfer coefficient and S is the 'structure factor' of the porous support, which is defined as

$$S = \frac{\tau\delta_m}{\varepsilon}, \quad (5)$$

with τ, ε and δ_m denoting the tortuosity, porosity and thickness of the support structure, respectively. It should be noted that eqn (4) is valid for the case where the membrane is oriented such that its porous support faces the feed stream (the biofuel mixture in the case considered herein). This is known to be a better choice in terms of the achievable permeation rate; however, it is also noted that under certain circumstances this orientation may have a higher propensity for fouling.[11] If it is further assumed that the membrane is in the spiral-wound configuration, the mass transfer coefficient may be calculated using the following correlation, based on CFD simulations and experimental measurements[13]

$$k = 0.065\mathrm{Re}^{0.875}\mathrm{Sc}^{0.25}\frac{D}{d_h}, \quad (6)$$

in which d_h is the channel's hydraulic diameter, $\mathrm{Sc} = \nu/D$ is the Schmidt number and $\mathrm{Re} = ud_h/\nu$ is the Reynolds number (of the

order of 100–400 in commercial spiral-wound modules), where u is the mean velocity in the channel and v is the fluid's kinematic viscosity. It should be noted that while this is indeed the current state-of-the-art configuration for osmotic membranes, other configurations, *e.g.* hollow-fibres, may become available in the future.

Finally, it is important to gauge the energy consumption of this process, which will primarily be due to viscous dissipation during the pumping of the two streams through the membrane module. An estimate of the dissipated energy may be made by computing the pressure drop at a given flow rate. In general,

$$\frac{\Delta P}{L} = C_{\mathrm{D}} \frac{\rho u^2}{2 d_{\mathrm{h}}}, \tag{7}$$

in which ΔP is the pressure drop, L is the channel length, ρ the fluid density and the drag coefficient in a spiral module is[13]

$$C_{\mathrm{D}} = 6.23 \mathrm{Re}^{-0.3} \tag{8}$$

The power requirement for the process is $\dot{P}_\gamma = \Delta p \cdot Q$, the product of the pressure drop and Q, the flow rate through the module. The latter is related to the average velocity *via* the available cross-sectional area of the module, *i.e.* $\mu = Q/n\varphi Wh$, where h and W are the single channel height and width, respectively, φ is the channel available volume fraction (since part of it is occupied by a mesh spacer) and n is the number of channels in the module. These parameters are taken here based on commercial spiral-wound elements (see ESI†).

Calculations of general process performance and, particularly, its energy consumption have been made by solving the system of eqn (1)–(3), supplemented by (4) and (6) for resolving internal and external mass transfer. While it is possible, in principle, to derive a local, differential version of these equations (resulting in a system of ordinary differential equations) there is little to be gained by this in the present analysis, which is aimed at a conceptual examination of the process potential. Therefore, all length varying parameters, *e.g.* concentrations and velocities, are taken as simple averages of inlet and outlet values. General parameters, characteristic of spiral-wound membrane modules, are given in the ESI,† along with other model parameters used in the calculations, such as solution properties. Key membrane properties are the water permeability and the structure factor, which are estimated based on values reported in the literature.[14–18] We note that the draw is here taken to be glucose, in a range of concentrations representative of a cellulosic source. Other sugars with possibly different draw characteristics may become relevant for future consideration.

Discussion

As an illustration of the osmotic permeation achievable using the available driving force, calculations have been made at different degrees of concentration (see Fig. 2). The base state is a system where no concentration (or dilution) is present, thus reflecting the maximum productivity of the process. A wider sensitivity analysis with respect to key process parameters, namely, the Reynolds number, which controls external CP; the membrane water permeability, dictating the efficiency of water transport for a given driving force and the structure factor, which affects the severity of internal CP, are given in the ESI.†

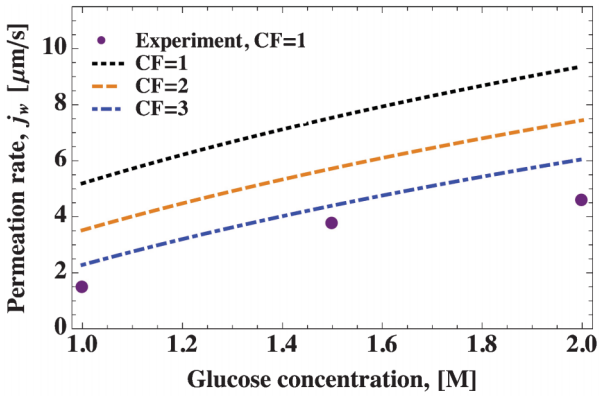

Fig. 2 Calculated (continuous lines) and measured (points) permeation rate as a function of the osmotic draw strength. Note: calculations made with C_B = 20 g L^{-1}, Re = 200, $A = 10^{-11}$ m s^{-1} Pa^{-1} and S = 200 μm, while in the experiments, $A = 2.5 \times 10^{-12}$ m s^{-1} Pa^{-1} and S = 600 μm.

Also shown in Fig. 2 is experimental data obtained from preliminary tests carried out using a custom-built bench-scale membrane unit (see schematic drawing in the ESI†). In these experiments, the permeation of water was measured during osmosis from a 20 g L^{-1} butanol solution into a 1–2 M glucose solution. A commercially available EO membrane (HTI) was used, while model calculations were made using parameters from improved membranes reported in the literature. This is the reason why measured permeation is lower than the model calculations. The projected permeation rate is encouraging, as it is comparable to that achieved in practice, for example, in reverse osmosis (RO) desalination.

Next, we consider the energy consumption used to pump the feed and concentrate streams. The energy dissipated within the membrane module is largely dependent on the hydrodynamic conditions which, for a given process feed stream (solution viscosity) and module geometry, is a function of the average (cross-flow) velocity. The calculated energy consumed per unit volume processed is shown in Fig. 3; besides the cross-flow velocity, other important parameters varied are the initially available osmotic driving force (*i.e.*, the glucose concentration) and the degree of concentration achieved. The latter has a profound effect on the required membrane area—since an increasing volume of water needs to be extracted to achieve higher concentration levels. Simultaneously, the available driving force is diminished, lowering the osmotic water flux and thus requiring more membrane area still. The cross-flow velocity has a seemingly opposite effect, albeit to a far lesser extent, since it promotes better mass transfer and, consequently, higher permeation rates. However, as the illustrative calculations show, these 'external' effects are not strongly limiting. Rather, increasing the cross-flow rate will result in a shorter residence time and, consequently, a larger membrane requirement or a multi-pass configuration. This obviously presents an

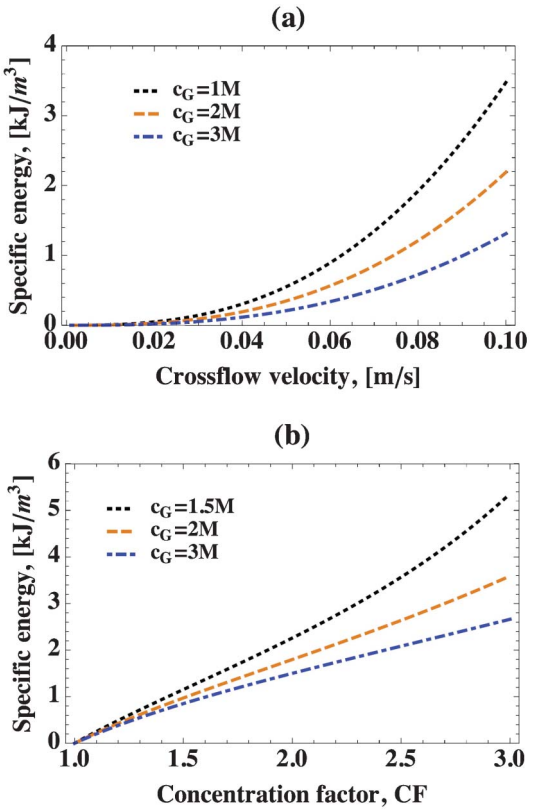

Fig. 3 The energy consumption of the osmotic pre-concentration step, shown for different initial glucose concentrations, representing the available osmotic potential. (a) the effect of increasing the crossflow velocity, at a two-fold concentration. (b) the effect of the degree of concentration at Re = 200. Note: calculations made for a C_B = 20 g L^{-1}, $A = 10^{-11}$ m s^{-1} Pa^{-1} and S = 200 μm.

optimization problem, since economical constraints must be taken into consideration and membrane area requirements are a good proxy for capital costs.

Concluding remarks

The main points to be drawn from these illustrative calculations may be summarized as follows. The energy consumption in the process is a small fraction of the energy offset from the downstream separation process. For example, the projected calculations estimate an energy consumption of ~1.6 kJ per cubic meter of processed fermentation feed, required for achieving a two-fold concentration using a 2 M glucose stock solution. This is less than one per cent of the energy offset which, in this case, is ~12 MJ (if distillation is used downstream). It is further illustrated that the membrane is the primary factor influencing process performance, through both the permeability and structure factor. Meanwhile, for a given osmotic potential, external mass transfer has a marginal influence on the permeation rate, within the range of Reynolds numbers of 50–500. This is an important observation since the Reynolds number, while increasing external mass transfer, comes at an energetic penalty through viscous dissipation within the channel. The effect of an increased concentration factor is reflected in a substantial loss of productivity. This should be borne in mind, as it will invariably affect process economics through an increased requirement for membrane area, which translates to larger capital expenditure.

Our preliminary tests have shown the commercial membrane achieved poor rejection, estimated to be ~40%. Further tests were carried out with commercial RO membranes (SW30, Filmtec), since this class of membranes has been reported to have a high rejection for ethanol and butanol.[19–21] However, our experiments showed that the membrane deteriorates over time (within hours), presumably due to differential swelling of the polyamide-based skin layer *vs.* the polysulfone support, resulting in delamination. This detrimental effect of butanol on the membrane was not reported in the previously published studies. Our test illustrates that at this point, there are no commercially available membranes suitable for this process. However, the great improvement of EO membranes achieved in recent years, combined with progress reported in fabrication of solvent-resistant membranes,[22–24] suggests that it should be feasible to fabricate a membrane with greater alcohol resistance, while possessing the structure of a membrane suitable for the EO process. Ultimately, it is demonstrated that the energy consumed in this process is a fraction of the energy offset through the introduction of a higher inlet concentration for the subsequent separation, whatever the method but particularly if distillation is used. Though much is still lacking in understanding the process viability, including economic considerations, its potential seems worthy of further investigation.

Notes and references

1 A. J. Ragauskas, C. K. Williams, B. H. Davison, G. Britovsek, J. Cairney, C. a. Eckert, W. J. Frederick, J. P. Hallett, D. J. Leak, C. L. Liotta, J. R. Mielenz, R. Murphy, R. Templer and T. Tschaplinski, *Science*, 2006, **311**, 484–9.
2 R. Luque, L. Herrero-Davila, J. M. Campelo, J. H. Clark, J. M. Hidalgo, D. Luna, J. M. Marinas and A. a. Romero, *Energy Environ. Sci.*, 2008, **1**, 542.
3 J. Goldemberg and P. Guardabassi, *Energy Policy*, 2009, **37**, 10–14.
4 W.-D. Huang and Y.-H. Percival Zhang, *Energy Environ. Sci.*, 2011, **4**, 784.
5 S. Atsumi, T. Hanai and J. C. Liao, *Nature*, 2008, **451**, 86–9.
6 M. Matsumura, H. Kataoka, M. Sueki and K. Araki, *Bioprocess and Biosystems*, 1988, **3**, 93–100.
7 T. C. Ezeji, N. Qureshi and H. P. Blaschek, *Curr. Opin. Biotechnol.*, 2007, **18**, 220–7.
8 L. M. Vane, *Biofuels, Bioprod. Biorefin.*, 2008, **2**, 553–588.
9 A. Oudshoorn, L. A. M. van der Wielen and A. J. J. Straathof, *Ind. Eng. Chem. Res.*, 2009, **48**, 7325–7336.
10 T. Cath, A. Childress and M. Elimelech, *J. Membr. Sci.*, 2006, **281**, 70–87.
11 S. Zhao, L. Zou, C. Y. Tang and D. Mulcahy, *J. Membr. Sci.*, 2012, **396**, 1–21.
12 K. L. Lee, R. W. Baker and H. K. Lonsdale, *J. Membr. Sci.*, 1981, **8**, 141–171.
13 G. Schock and A. Miquel, *Desalination*, 1987, **64**, 339–352.
14 A. Tiraferri, N. Y. Yip, W. A. Phillip, J. D. Schiffman and M. Elimelech, *J. Membr. Sci.*, 2011, **367**, 340–352.
15 G. Z. Ramon, B. J. Feinberg and E. M. V. Hoek, *Energy Environ. Sci.*, 2011, **4**, 4423.

16 C. Qiu, L. Setiawan, R. Wang, C. Y. Tang and A. G. Fane, *Desalination*, 2012, **287**, 266–270.
17 P. Sukitpaneenit and T.-S. Chung, *Environ. Sci. Technol.*, 2012, **46**, 7358–65.
18 N.-N. Bui and J. R. McCutcheon, *Environmental science & technology*, 2013.
19 a. Garcia, E. L. Iannotti and J. L. Fischer, *Biotechnol. Bioeng.*, 1986, **28**, 785–91.
20 C. Schutte, *Desalination*, 2003, **58**, 285–294.
21 N. Aydogan, T. Gurkan and L. Yilmaz, *Sep. Sci. Technol.*, 2005, **39**, 1059–1072.
22 D. Bhanushali and D. Bhattacharyya, *Ann. N. Y. Acad. Sci.*, 2003, **984**, 159–177.
23 J. Geens, K. Peeters, B. Vanderbruggen and C. Vandecasteele, *J. Membr. Sci.*, 2005, **255**, 255–264.
24 P. Vandezande, L. E. M. Gevers and I. F. J. Vankelecom, *Chem. Soc. Rev.*, 2008, **37**, 365–405.